

Review

## Nano and Microscale Topographies for the Prevention of Bacterial Surface Fouling

Mary V. Graham and Nathaniel C. Cady \*

State University of New York (SUNY) College of Nanoscale Science & Engineering, 257 Fuller Road, Albany, NY 12203, USA; E-Mail: mgraham@albany.edu

\* Author to whom correspondence should be addressed; E-Mail: ncady@albany.edu;  
Tel.: +1-518-956-7354.

Received: 13 November 2013; in revised form: 20 December 2013 / Accepted: 8 January 2014 /  
Published: 17 January 2014

---

**Abstract:** Bacterial surface fouling is problematic for a wide range of applications and industries, including, but not limited to medical devices (implants, replacement joints, stents, pacemakers), municipal infrastructure (pipes, wastewater treatment), food production (food processing surfaces, processing equipment), and transportation (ship hulls, aircraft fuel tanks). One method to combat bacterial biofouling is to modify the topographical structure of the surface in question, thereby limiting the ability of individual cells to attach to the surface, colonize, and form biofilms. Multiple research groups have demonstrated that micro and nanoscale topographies significantly reduce bacterial biofouling, for both individual cells and bacterial biofilms. Antifouling strategies that utilize engineered topographical surface features with well-defined dimensions and shapes have demonstrated a greater degree of controllable inhibition over initial cell attachment, in comparison to undefined, texturized, or porous surfaces. This review article will explore the various approaches and techniques used by researchers, including work from our own group, and the underlying physical properties of these highly structured, engineered micro/nanoscale topographies that significantly impact bacterial surface attachment.

**Keywords:** topography; bacteria; biofouling; biofilm; surface; attachment; antifouling; nanotechnology; nanofabrication

---

## 1. Introduction

### 1.1. Overview

Bacteria inhabit nearly every type of environment and can be found in air, water, and, most notably, on surfaces. Surface associated bacterial attachment and growth is mediated by a wide range of adhesion and growth mechanisms, which often result in the establishment of bacterial aggregates, known as biofilms. Surface attachment and subsequent biofilm formation are a type of “biofouling”, which can be defined as the accumulation of biological matter on material surfaces. While bacterial biofouling can be beneficial under some circumstances, such as in biologically-based wastewater treatment systems, most biofouling can be detrimental or even damaging to the system in question. Much work has been dedicated to preventing or mitigating bacterial biofouling, most notably in the fields of medical devices, transportation (primarily in the maritime industry), and in the food industry. In our own research group, we have focused primarily upon prevention of biofouling for medical devices, since device-associated fouling by pathogenic bacteria can lead to disease and in severe cases mortality. This review highlights early work on microorganism fouling of roughened and texturized surfaces, then expands to include recent work on engineered surface topography for antifouling purposes. We also explore some of the mechanisms behind the antifouling properties of topography at the micro and nanoscale levels.

### 1.2. Surface Attachment and Biofilm Formation

Biofouling by microorganisms begins with initial attachment and adhesion to surfaces, typically followed by growth and expansion into a biofilm. Biofilms are structured communities of microbial cells embedded in extracellular polymeric substances (EPS) [1–3]. EPS is primarily composed of polysaccharides, nucleic acids, proteins, and other secreted substances which encase the constituent cells and often render them resistant to mechanical removal, host immune responses, and antibiotic therapies [1–4]. Given that biofilms exhibit increased resistance to removal and susceptibility to chemical or antibiotic treatments [5], prevention during the primary attachment phase is desirable. In this initial stage, cell-surface attachment is thought to be a partially reversible process as attachment can be more readily disrupted than during later stages of biofilm formation [6]. The key to this strategy is finding methods to prophylactically treat surfaces to limit the initial attachment of freely floating (planktonic) cells that attach to surfaces via various strategies, including adhesion proteins, appendages, and through the excretion of EPS. Bacterial attachment at this initial stage is, by all means, a complex process that is governed by multiple cell-surface interactions. These interactions can be greatly influenced by surface chemistry (functional groups, electrostatic charge, coatings), surface energy (as related to the surface hydrophobicity), mechanical properties (elastic modulus, shear forces), environmental conditions (pH, temperature, nutrient levels, competing organisms), surface topography, as well as bacterial surface structures (pili, flagella, fimbriae, adhesins) [7–18]. Cell attachment to surfaces is governed by a combination of all these factors (surface properties, environmental conditions, and cell physiology), making it virtually impossible to uncouple the influence of individual factors. However, there is merit in studying individual factors to better understand the entire process of biofouling.

### 1.3. Biofouling of Medical Devices

Bacterial biofouling on the surfaces of indwelling medical devices is a leading cause of device-related infection and disease. Reports show that in the United States alone, over half of the two million cases of nosocomial infections that occur yearly are associated with indwelling medical devices [18]. Annual studies show that catheters account for hundreds of thousands of infections, resulting in a both a significant cost and burden to the present healthcare system [18]. The surfaces of many implanted devices are designed to encourage soft- and/or hard-tissue adherence [19]. Consequently, these surfaces also serve as an opportune substrate for bacteria to colonize and eventually form biofilms [20]. Both acute and chronic infections are associated with biofilm-infected devices. Such infections can even have periods of latency, followed by unexpected resurgence events, triggered throughout the patient's lifetime [21]. Pathogens contaminate indwelling medical devices through a multitude of exogenous pathways. Foreign bacteria can be transferred to device surfaces via cross-contaminated surgical instrumentation, during surgical preparation procedures, and even during device placement [21]. Alternatively, host-associated bacteria can colonize implanted devices post-surgery. Colonization by host-associated bacteria can occur weeks to months post-implantation, often resulting in latent infections [21]. Device colonization via either route is often followed by the formation of biofilms, which exacerbates removal or remediation, and often renders bacteria resistant to antibiotic therapies [22]. This can lead to systemic infection or disease, which can ultimately result in mortality if the host remains septic. Devices that are commonly associated with biofilm-forming bacteria include non-surgically implanted devices (*i.e.*, contact lenses, endotracheal tubes, and urinary and central venous catheters) as well as permanently implanted devices (*i.e.*, cardiac valves, vascular grafts, plastic surgery augmentation devices, and joint replacements) [21,23]. Various pathogens have been implicated in device related infections including *Escherichia coli*, *Staphylococcus aureus*, *Staphylococcus epidermidis*, *Pseudomonas aeruginosa*, *Pseudomonas fluorescens*, *Listeria innocua*, and *Enterococcus faecalis*.

Preventing bacterial attachment to surfaces is critical for the reduction of infections associated with indwelling biomedical devices. Multiple avenues have been explored as a means to combat this issue, including the use of various antibiotic therapies, drug delivery methods, and surface coatings [21,24–30]. Though the efficacy of these methods has proven substantially affective, they remain limited in their long-term effectiveness. Many of these surface coatings and devices that have been loaded with time-release antibiotics are in quintessence very transient and deplete over time [8,31–33]. Additionally, studies have shown that bacteria can develop increased resistance to antibiotic treatments and antibacterial coatings, essentially rendering them ineffective [34–36]. While there remains a facet of variables and conditions that can be used in tandem and fine-tuned to produce optimal antifouling surfaces, there still remains a need to uncover a more persistent strategy.

### 1.4. Using Topography to Inhibit Attachment and Biofouling

Cellular interactions with surfaces are governed by multiple facets, including the surface chemistry, surface charge, surface mechanical properties, and topographical structure. Under most circumstances, surface topography is controlled at the macro-scale (micrometer size scale and larger) but is not highly controlled at the micro- and nano-scale. Most bacterial cells are in the micrometer size range, while their

surface appendages are in the nanometer size range. Thus, control of surface topography in the nanometer to micrometer size range could play a pivotal role in bacterial attachment and subsequent biofouling and biofilm formation. Multiple research groups have adopted this hypothesis and have been exploring topography as a key parameter for development of antifouling surfaces. While engineering surface topography has not been as extensively explored as some of the other aforementioned strategies, it has advantages including non-toxicity (which reduces the potential for medical complications/incompatibilities) and is independent of material type (assuming that the material can be molded or fabricated to present engineered topographies with high fidelity). Many groups have fabricated engineered surface topography, using numerous fabrication techniques (soft lithography and double casting molding techniques, microcontact printing, electron beam lithography, nanoimprint lithography, photolithography, electrodeposition methods, *etc.*) [37–47] on a wide range of substrates, ranging from various polymeric materials (silicone, polystyrene, polyurethane, and epoxy resins) to metals and metal oxides (silicon, titanium, aluminum, silica, and gold) [21,40,45,47–55]. Furthermore, engineered topography can be considered as part of a multi-faceted strategy to prevent biofouling, and could be combined with other methods such as surface chemical treatments, addition of antibiotics/bacteriostatic agents, *etc.* [56,57].

Early studies that explored the effects of surface topography on biofouling focused on surface topographies that were generated through mechanical processing methods, roughening, or polishing techniques [58]. On these surfaces, residual bacterial cells were observed to be wedged tightly between randomly sized grooves and cavities. Moreover, the presence of narrow grooves and cavities was shown to exacerbate the bacterial cell removal process, most notably on food processing equipment [59]. In a similar study, surface topographies that consisted of “random texturized roughness” assisted in the retention of bacteria cells and promoted colonization and contamination [60].

More recently, several groups have shifted focus toward the use of engineered surface topographies that could be scaled and tailored to prevent fouling by specific organisms or classes of organisms. The general hypothesis of these studies is that topographies with defined feature dimensions (*i.e.*, shape, height/depth, width, length) and spacings can be specifically scaled in accordance to target organisms to ultimately restrict and inhibit movement of motile cells and limit the surface area contact the cell is able to make with the surface. By adding control over the structure of the surface features, one can drastically limit initial bacterial attachment, thus reduce colonization and biofilm formation.

In this review article, we largely focus on surveying recent works using engineered surface topographies, and investigating the possible underlying physical properties of micro- and nanoscale topographies which render them essential for the fabrication of antifouling surfaces.

## **2. Micron-Scaled Engineered Surface Topography for Inhibition of Biofouling**

### *2.1. Early Work: The Influence of Microtopography on Biofouling*

Initial research in the food industry laid much of the groundwork for current efforts to engineer surfaces that could reduce the attachment and proliferation of bacteria. Contamination of food preparation surfaces and food processing machinery is particularly problematic, especially when bacteria are persistent or resistant to chemical disinfectants or mechanical cleaning processes [17]. For instance, it is not uncommon to find bacterial organisms inhabiting industry standard stainless steel

surfaces where food products are routinely handled. In general, as long as the surface remains in sound, hygienic conditions, bacterial contaminants can be safely removed from the surface, via common industry standard practices, to meet regulation standards. However, with continued use, these surfaces undergo degradation and exhibit normal wear resulting in minor defects, scratches, and voids. Mechanically worn and damaged surfaces were shown to trap bacterial cells between narrow grooves, pits, and cracks. Ultimately, this presents challenges in effective cleaning and removal, as bacteria trapped in these regions are difficult to reach or dislodge using normal cleaning practices. Thus, improving our understanding of the mechanics behind cell-substratum retention may help establish useful strategies to remedy this issue.

Whitehead *et al.* made observations on how the shape of the surface features is essential for understanding the effects of bacterial cell retention [58]. They observed three main cell retention characteristics: (1) When surface grooves are in close proximity to one another, with distances smaller than bacterium dimensions, there may be minimal cell-substratum interaction; (2) As grooves become wider (on the size scale of individual cells) microorganisms are able to fit between grooves, thus forming enhanced cell-substratum contact. It is believed that this increases the binding energy and promotes the propensity of microorganism retention on the substratum surface; (3) On wider spaced grooves (greater than the size of individual cells) there is minimal cell-substratum contact because from the point of reference of the microorganism, it does not appear to experience roughness created from surface defects. In this regime, cells are hypothesized to encounter a surface that appears smooth. From these observations, Whitehead *et al.* deduced that surface cleanability has a direct correlation to substratum wear, as microorganisms take refuge in various surface defects [58]. They hypothesized that surface roughness (from the contribution of surface wear) plays a pivotal role in cell retention.

Cell retention on surfaces is complex, as there is an intricate interplay of multiple variables that require further exploration. Controlling these factors should help us to gain a more concise understanding of how surface features and cell retention correlate so that strategies could be adopted to build upon this initial body of knowledge. This has become extremely significant for more recent work involving the use of engineered topography as a means of fabricating antifouling surfaces. Whitehead *et al.* [58] established a practical connection between the relevance of the size scale of an organism of interest, and the necessary size dimensions needed for the topographical features to reduce fouling by that organism. In the subsequent sections of this review we highlight research that has adopted this engineering strategy (tailoring antifouling surfaces to specific organisms, based on organism size and shape). We begin by discussing relevant works from marine biofouling and expand to other applications, such as for medical devices. While we aim to extensively cover engineered antifouling topographies, we recognize that this field is still relatively new and, as such, does not have the breadth of publications as more mature fields.

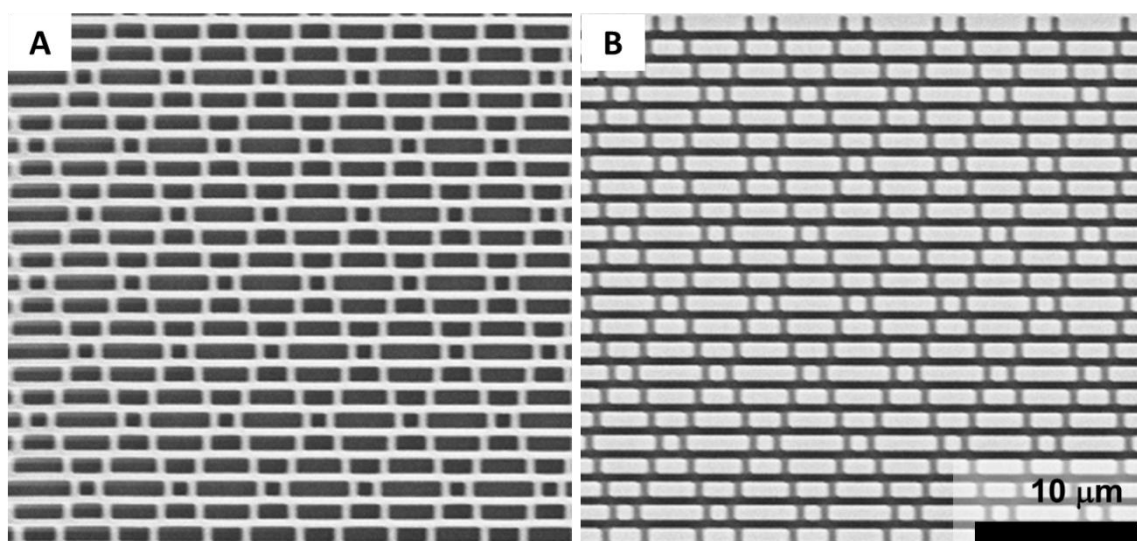
## 2.2. Microtopography Applied to Marine Biofouling

Beyond the food industry, biofouling is particularly problematic for the maritime industries. Aquatic microorganisms accumulate on the surfaces of seagoing vessels, increasing fuel consumption due to excess drag forces. In addition, biocorrosion processes can result in loss of hull strength, or even more drastically, breaches in the hull structure, resulting in costly repairs [61]. There is a wide diversity of marine biofouling culprits, including fungi, protozoa, algae, and invertebrates. Typical strategies for

preventing or treating marine biofouling include the use of toxic paints and coatings, and repeated mechanical cleaning procedures. Frequent cleaning is costly and time consuming, while the use of toxic paints and coatings can have environmental consequences, and many coatings are therefore under scrutiny by regulatory agencies such as the Environmental Protection Agency (EPA). Thus, finding non-toxic schemes that comply with environmental concerns has led to the development of engineered topographical surface features that exhibit antifouling properties [62].

In several publications, Schumacher *et al.* described a biomimetic approach to designing antifouling topographies [14,61,63]. In these works, engineered topographical surfaces, fabricated from silicone elastomer, were used to reduce the attachment of algal spores (*Ulva spp.*). Topographical features that were explored included smooth (*i.e.*, no topography) control surfaces, linear ridges (2  $\mu\text{m}$  wide features separated by 2  $\mu\text{m}$  wide channels), hexagonally packed circular pillars (2  $\mu\text{m}$  diameter), equilateral triangles (10  $\mu\text{m}$ ) combined with circular pillars (2  $\mu\text{m}$  diameter), and lastly the Sharklet AF™ design (consisting of 2  $\mu\text{m}$  ribs of lengths 4, 8, 12, and 16  $\mu\text{m}$ ). Each of the topographical patterns showed reduced attachment by *U. linza* spores, *vs.* a smooth, undefined surface. Furthermore, the Sharklet AF™ design had the highest antifouling efficacy. In fact, our laboratory has fabricated silicone replicas of the Sharklet AF design in both its original form, and an “inverted” design (Figure 1). As the name suggests, Sharklet is a biomimetically inspired design based upon the microbial resistant skin of fast swimming sharks. To date, it has gained much commercial appeal for a wide range of useful applications. But what qualities make it such an effective antifouling topography?

**Figure 1.** Electron micrographs of engineered topographies for antifouling purposes. A copy of the biomimetic “Sharklet AF” pattern [61], fabricated by the authors, is shown. The topography was replicated in recessed form (A) in which the short repeating lines are three-dimensional depressions, and in a raised form (B) where the short repeating lines project out of the surface.



Multiple hypotheses have been formulated regarding the mechanisms by which Sharklet AF™ resists microorganism attachment [64,65]. Bhushan’s work on bioinspired structured surfaces sheds light on some of the mechanics behind its efficacy [64]. Fast swimming sharks possess multipurpose skin that

facilitates drag reduction by secretion of a protective mucus layer, and through the three dimensional topography of small structures on its skin. The element of their skin that has been shown to be most effective at reducing microbial attachment is the presence of tiny scales, known as dermal “denticles” (skin teeth), which cover its body. The denticles are composed of small “riblets” that are aligned in the direction of fluid flow. The unique size and spacing between the “riblets” appear to prevent microorganism attachment (such as the approximately 5–10  $\mu\text{m}$  diameter spores of *Ulva spp.*). Bhushan describes other optimized implementations of this “riblet” feature [64]. They include the sawtooth, scalloped, and blade geometries. When comparisons are made between the three varieties in terms of optimal drag reduction, blade riblets proved to exhibit the greatest degree of drag reduction, followed by scalloped riblets, and lastly sawtooth.

Expanding upon their highly effective, antifouling Sharklet design, the Schumacher group has explored variations on this theme. Their basic premise is that topography-based antifouling surfaces have greater efficacy when the size regime of the fouling organism of interest is taken into account. Since microorganisms have a wide range of external dimensions, surface topographies that contain only one length scale may not prove to be efficient as a universal antifouling marine coating. It becomes crucial to develop a group of topographical patterns that can limit surface attachment by organisms with variable size and morphology. To this end, the authors developed a hierarchical strategy that superimposed smaller anti-algal topography (Sharklet design with an aspect ratio of 2) onto larger anti-barnacle topography (ridges with 40  $\mu\text{m}$  feature height) [14]. Their results showed a 97% reduction in microorganism attachment. While hierarchical topographical features may provide increased antifouling efficacy, they can be difficult to fabricate. Traditional polymer molding techniques are dependent upon high-precision molds. Creating hierarchical features in such molds can be difficult, necessitating alternative approaches such as two-step molding or grafting of smaller features onto the molded substrate after the base molding is completed. For these reasons and others, hierarchical designs have not been fully exploited for antifouling purposes.

The Schumacher group has also explored the role that micro-feature aspect ratio (ratio of feature height and/or depth to the feature’s lateral dimensions/width) plays in cell retention. They argue that besides the size (diameter, length, *etc.*) of the fouling microorganisms, the size and function of their settlement sensory organs, which probe and navigate in search of an ideal location, must be taken into consideration. Using the Sharklet topography, they investigated attachment behavior on surfaces with varying features heights (1, 2, and 3  $\mu\text{m}$ ) [14]. Their findings demonstrate that there is a significant correlation between aspect ratio and antifouling efficacy. As the aspect ratio was increased by one unit, attachment was significantly reduced by 42%–45%.

### 2.3. Approaches for Predicting Antifouling Efficacy for Microtopographical Surfaces

The biomimetic strategy employed by Schumacher *et al.* to generate the Sharklet topography demonstrates an effective approach for creating antifouling surfaces that inclusively takes into account the role of hierarchical design on multispecies biofilm formation, as well as the influence aspect ratio has on attachment of microorganism appendages. This approach is limited, however, by the ability to find unique organisms or surfaces that are inherently antifouling, or by the ability to modify such surfaces to increase their antifouling properties. Thus, one of the next logical steps is to find predictive methods to

draw correlations between a topographical pattern and its ability to reduce cell attachment. Schumacher *et al.* have formulated two methods to address this: (1) the engineered roughness index (ERI); and (2) the nanoforce gradient.

The engineered roughness index (ERI) is a dimensionless value used to characterize surfaces with engineered topographies. The formula, shown in Equation (1), is based solely on three parameters associated with the geometry, spatial arrangement, and size of the topographical features. These include Wenzel's [66] roughness factor ( $r$ ), depressed surface fraction ( $f_D$ ), and degree of freedom of movement ( $df$ ) [61].

$$\text{ERI} = (r \times df)/f_D \quad (1)$$

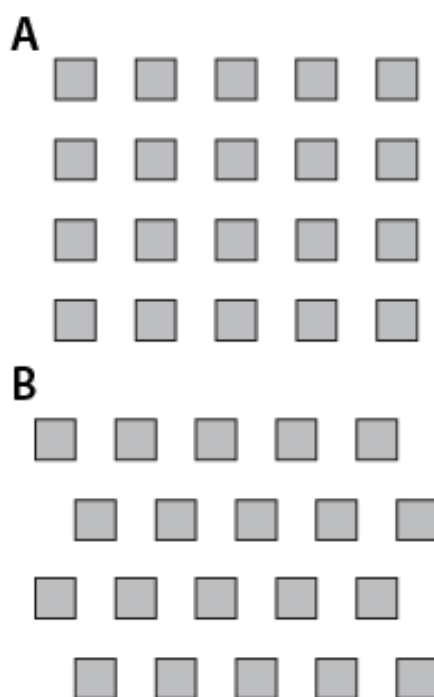
A more detailed description of each parameter can be found in the relevant citations [66–71]. But as described in Schumacher *et al.* [61], Wenzel's roughness factor ( $r$ ) is defined as the ratio of the actual surface area to the projected planar surface area. The actual surface area encompasses the entire area spanning the feature tops, feature sidewalls, and depressed areas (floors) between features. The projected planar area therefore encompasses only the feature tops and depressions/floors (no sidewalls). The depressed surface fraction ( $f_D$ ) is described in Schumacher *et al.* [61] as being the ratio of the recessed surface area between the protruded features and the projected planar surface area (as previously described above). Schumacher *et al.* state that this depressed surface fraction term is equivalent to both  $1-\phi_S$  and  $1-f_1$ , where  $\phi_S$  is the surface solid fraction as detailed by Bico, Quéré and colleagues *et al.* [67–69,71]. The  $f_1$  factor refers to the solid-liquid interface term of the Cassie-Baxter relationship for wetting [70]. The final term, the degrees of freedom for movement ( $df$ ), is described in Schumacher *et al.* [61] as relating to the tortuosity of the surface and the ability of an organism to follow recesses (*i.e.*, grooves or depressed areas) between features within the topographical surface. For example, if the recessed area forms a continuous, intersecting grid, allowing movement within the  $x$  and  $y$  plane, then  $df$  equals 2. Alternatively, if the recessed areas resembled an array of linear trenches, restricting movement to, say, the  $x$  plane, the  $df$  will equal 1.

Schumacher *et al.* showed an inversely proportional correlation between microorganism attachment density and ERI value. Thus, out of all their tested surface topographies (smooth, ridges, hexagonally packed (HP) pillars, equilateral triangles surrounded by HP pillars, and the Sharklet topography) the Sharklet pattern had the highest ERI value, and consequently the lowest cell attachment density. To date, there have been further adaptations to the ERI concept in order to optimize its formula [72].

Although the ERI model is quite informative in correlating predicted attachment behavior amongst a settling microorganism and a topographically defined surface comprised of engineered features, our group has shown that it is not devoid of limitations [73]. While we found that the ERI value correlates well to attachment for a subset of the features we have tested, that correlation appears to be restricted to only a range of feature sizes. As our features approached relative smoothness (either toward very small feature size or toward very large feature size) the ERI was unable to predict cell attachment accurately. It is important to note that the ERI encodes no notion of scale. The ERI does not capture the relationship between effective feature size and organism size. Rather, the ERI relies on the investigator to constrain their range of exploration to surface topographies comprised of features of similar relative scale to the organism of interest. Without the notion of scale the ERI can only be relied upon as a general indicator of the topography's antifouling efficacy. The ERI cannot be used to optimize a surface topography for a

particular organism or set of organisms. For example, optimizing the ERI for a surface of pillars with 2 “degrees of freedom” results in a relatively smooth surface where the pillars are placed as close to each other as the resolution of the fabrication process allows. Furthermore, the ERI cannot make a significant distinction between certain sets of features. As a simple example, according to calculation of the ERI, there is no distinguishable difference between an evenly spaced grid of squares and an offset grid arrangement as shown in Figure 2. Meanwhile, cell attachment density on both of these differently arranged surfaces proves that there are major differences in degrees of attachment. Thus, although the ERI formulation can be quite predictive in many aspects, it is not sufficient for predicting all cell attachment scenarios. In order to enable the optimization of the design of these surfaces, new characterizations must be investigated which capture more descriptors of the surface and the surface-organism interaction.

**Figure 2.** The two grid arrangements, (A) normal grid arrangement and (B) grid arrangement with a slight offset, are largely indistinguishable by the Engineered Roughness Index (ERI) From Graham *et al.* [73], reproduced by permission of The Royal Society of Chemistry.



The other predictive approach, which calculates so-called “nanoforce gradients”, comes as a direct effect of surface topography and substratum mechanics [63]. It explores the mechanical forces exerted on and sensed by an attaching microorganism. The underlying phenomenon is known as mechanotransduction, which is a concept that has been extensively explored for cell and tissue engineering applications. The authors state that most strategies have not actively taken on the consideration of this principle in the overall design and modeling of antifouling surfaces [63]. In their work, the authors developed surface topographies in which individual organisms could interact with surface features having differential “bending moments”. Varying the size and/or cross-section of adjoining surface features resulted in a differential force needed to bend or move the adjoining features during microorganism settling and attachment. The authors estimated the lateral force required to cause 10% deflection of individual

features using Equation (2), below, in which  $F$  is the applied force,  $E$  is the modulus of elasticity,  $I$  is the rectangular moment of area,  $L$  is the height of the feature, and  $y$  is the end deflection distance:

$$F = \left(\frac{3EI}{L^3}\right)y \quad (2)$$

Using this equation and associated model, the authors designed topographical patterns in which neighboring features had relative force gradients (bending force differential between features)  $> 100$  nN. A variety of such “nanoforce gradient” surfaces were explored. The experimental work also included a smooth surface (positive control) as well as the Sharklet design (negative control). Their findings showed an inversely proportional relationship between attachment and the calculated nanoforce gradient, such that surfaces with higher nanoforce gradients exhibited lower cell attachment. Further, the smooth surface had the highest cell attachment, while the Sharklet pattern showed the lowest cell attachment of any of the patterns tested. In efforts to explain why the Sharklet design once again outperformed the other topographically defined surfaces, the authors state that it could be due to the complex four-element engineered topography, which presents more tortuosity (the ability for the cells to follow bends and recesses associated with the surface features).

#### 2.4. Modes of Bacterial Surface Attachment/Alternative Topographies

Most of the studies described in this review utilize some form of microfabrication and/or direct patterning of surface topography. Most of these approaches result in highly regular surface structures with a square or rectangular cross-sectional profile. Kargar *et al.* introduced an alternative approach to antifouling surfaces by fabricating topographical features with curved tops, instead of the more typical flat-topped, rectangular profile features [52]. To fabricate these curved surface topographies, smooth polystyrene (PS) surfaces served as a substrate for a network of linearly arranged PS fibers. The highly aligned fibers were deposited onto the substrate via a non-electrospinning method known as the Spinneret based Tunable Engineered Parameters (STEP) technique [74]. The authors mention that fibers were selected as a texturizing agent for the surface, primarily because they are not flat, and could enable the exploration of the effect of surface curvature. From their experimental results they observe four dominant modes of attachment behavior between the cell and the substratum topography: (1) AS (cell is aligned with spacing); (2) CS (cell has crossed the spacing); (3) CF (cell has crossed the fiber); and (4) AF (cell is aligned with fiber).

In another departure from standard microtopographies, Perni *et al.* investigated the antifouling properties of microscale conical structures [75]. Using laser ablation, cone-shaped holes were formed on silicone substrates, and then filled with curable silicone to produce polymeric replicas. The resulting replicas contained cones with base diameters of 20, 25, 30, and 40  $\mu\text{m}$ , with corresponding depths of 1, 2, 6, and 9  $\mu\text{m}$ . Using *E. coli* and *S. epidermidis*, bacterial attachment to these surfaces was assessed. Their results revealed that for both bacterial species, cells preferred to settle and attach to the floor of the surface, and not to the top of the cone structures. This is similar to our group’s observation that cells tend to attach to the spaces between projecting features, if the space between features is equal to, or larger than the width of the cells. Clearly, more work needs to be performed in order to compare cell attachment to curved structures and sharpened, cone-like structures, as opposed to structures with a rectangular profile.

### 2.5. Microtopography to Prevent Fouling of Medical Devices

Moving beyond marine biofouling, we now redirect our focus to the biomedical arena, where the surface-fouling microorganisms of interest are considerably smaller in size (typically 1–2  $\mu\text{m}$  vs. 5–10  $\mu\text{m}$  or greater in marine environments). Chung *et al.* have adapted the successful Sharklet topographical design in efforts to explore its efficacy in the area of bacterial biofouling on the surfaces of indwelling medical devices [76]. This group was primarily interested in preventing the attachment of *Staphylococcus aureus*, an opportunistic organism associated with a host of nosocomial infections. Methicillin-resistant *Staphylococcus aureus* (MRSA) causes infections that are extremely difficult to treat in humans due to its ability to form biofilms, and its natural resistance to multiple antibiotics [77]. The authors were interested in determining if the Sharklet antifouling topography, which has made tremendous strides in the area of marine biofouling, would be just as effective at bacterial biofouling. They analyzed *S. aureus* biofilm growth on smooth surfaces (the control group) and surfaces that were topographically defined with the Sharklet pattern (having the same feature dimensions as previously described). The experiments showed significant disruption of bacterial biofilm in the presence of topography *versus* a smooth, unpatterned surface. However, cells (and biofilm) were observed in the recessed areas between features in the Sharklet pattern. This indicates the ability of *S. aureus* to attach to the Sharklet pattern, and limits the long-term usefulness of this topography, since the attached bacteria/biofilm could eventually expand to cover the entire surface.

Reddy *et al.* have also explored bacterial biofouling using the original Sharklet design [78]. However, in their study, a different pathogenic microorganism was surveyed. The authors examined catheter-associated urinary tract infections (CAUTI) caused by uropathogenic *Escherichia coli*. This is one of the most common device-related infections, which can give rise to serious medical complications [79]. Their interest was in exploring the effects the surface microstructures of the Sharklet design had on bacterial colonization and migration. This group performed cell attachment assays on three different Sharklet design variations: (1) raised topography (2  $\mu\text{m}$  feature widths with 2  $\mu\text{m}$  spaces); (2) recessed topography (2  $\mu\text{m}$  feature widths with 2  $\mu\text{m}$  spaces); and (3) raised topography (10  $\mu\text{m}$  feature widths with 2  $\mu\text{m}$  spaces). A smooth (*i.e.*, no topography) surface was included in the assay as a control. Cell attachment experiments showed that all three variations of Sharklet designs outperformed the smooth surface, with an average reduction of 47% in colony forming units (CFUs) and bacterial area coverage.

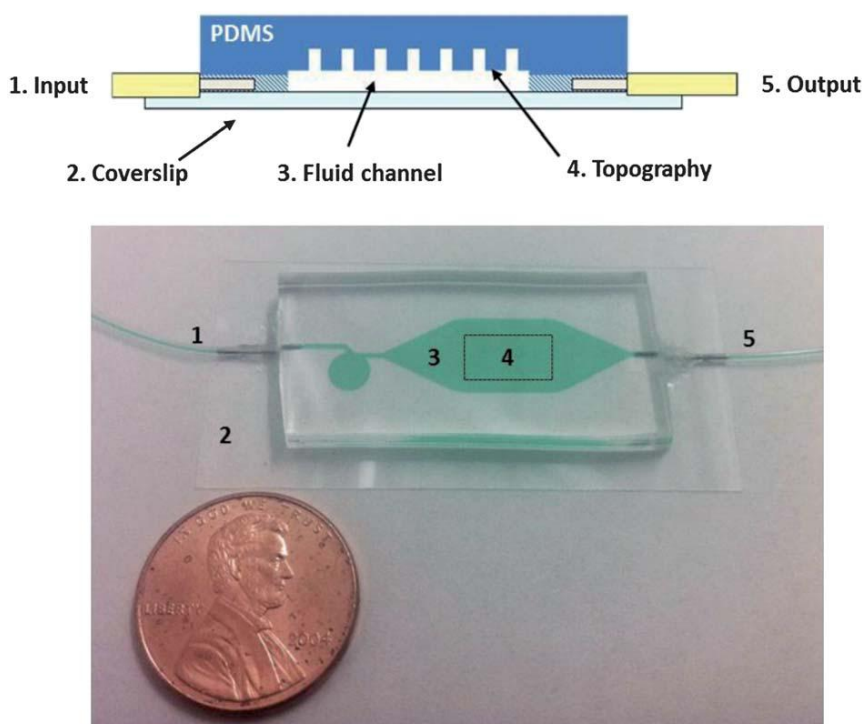
Given that the Sharklet design has proven effective for marine applications, it comes as no immediate surprise that researches would explore its effectiveness for biomedical applications. One outstanding question, however, is whether or not the Sharklet design is scalable, and able to retain antifouling efficacy for smaller organisms when scaled to 0.5–2.0  $\mu\text{m}$  feature dimensions. At the time of this review, no publications have described fabrication or testing of scaled Sharklet patterns for antifouling purposes. However, similar to the biomimetic approach taken by Schumacher *et al.* Epstein *et al.* have investigated a bioinspired, dynamic surface design that is built upon the strategy of mechanical frustration of sedentary marine organisms, commonly known as echinoderms [80]. The antifouling surfaces of echinoderms (*i.e.*, sea urchins and starfish) was adapted and modified into a more simplistic form of a uniaxially stretching elastic surface. These organisms have skin that is densely packed with mobile, spiny microstructures known as pedicellaria. These perpetually moving structures on the skin prevent the settlement and adherence of various microorganisms. In the bioinspired adaptation of this

phenomenon, Epstein *et al.* fabricated topographically defined surfaces, resembling highly controlled wrinkles with troughs that were intentionally tuned to be either (1)  $<1\ \mu\text{m}$  wide; (2)  $\sim 1\ \mu\text{m}$  wide; or (3)  $\sim 2\ \mu\text{m}$  wide. To make these wrinkled substrates dynamic, a 20% pre-stretch was applied during an oxidation step. Upon relaxation, the substrate surface exhibited highly controlled, regular buckling. Experimental assays, using *P. aeruginosa*, *S. aureus*, and *E. coli*, were performed on a smooth surface (as a control), and the wrinkled surfaces. Results showed biofilm inhibition on the topographically defined, wrinkled surfaces, yielding a new paradigm for fabrication of antifouling surfaces.

### 2.6. Antifouling Microtopography under Fluid Flow Conditions

Multiple studies have examined cell attachment to surfaces under static (non-dynamic) fluid conditions. In our group, we have explored the effects of fluid flow on bacterial surface attachment, within microfluidic devices. The goal of this work was to better understand how microscale topographic features affected cell attachment under both dynamic and static conditions. Utilizing an array of different surface topographies (including line/space patterns and micrometer-scale holes), we surveyed bacterial cell attachment under static (cell settlement due to gravitational effects) and laminar flow conditions using a custom-fabricated microfluidic device (Figure 3) [73].

**Figure 3.** Microfluidic device used for bacterial surface attachment studies under dynamic fluid flow conditions (from Graham *et al.* [73], reproduced by permission of The Royal Society of Chemistry).

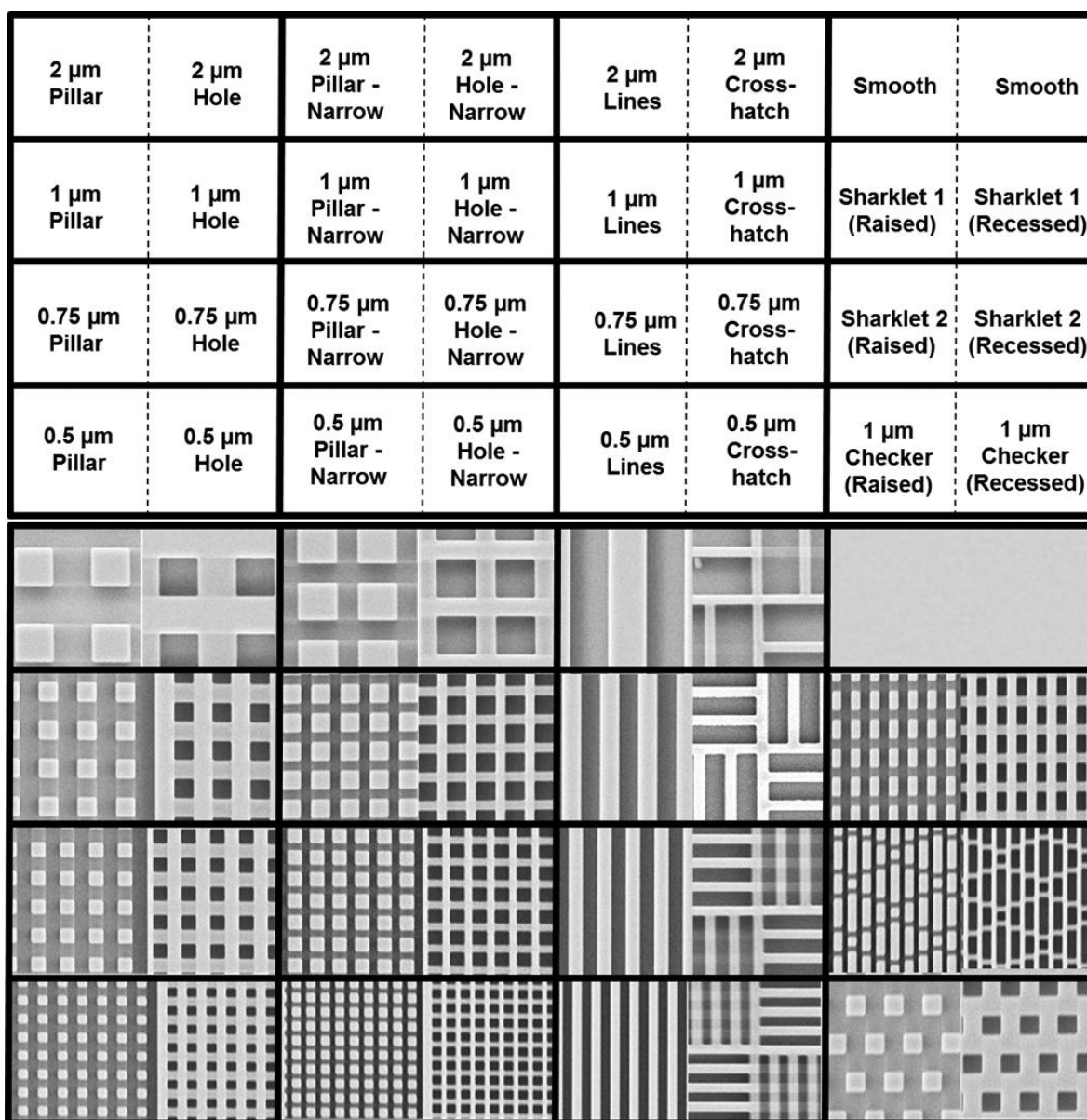


In the case of our fluid flow studies, we placed our microfluidic device in two distinct orientations, (1) so that the bacterial cells were flowing above the topographical features; and (2) so that the bacterial cells were flowing below our topographical features. We also performed attachment studies under static conditions (without fluid flow). Despite differences in the overall magnitude of cell attachment, results

for all three conditions (topography “up”, topography “down”, and static) showed similar trends, in that cell attachment was significantly reduced on topographically defined surfaces, vs. a smooth (control) surface. Furthermore, within our topographically defined structures, the spacing between features dictated cell attachment density (with fewer cells attaching to feature sets with narrower spacing).

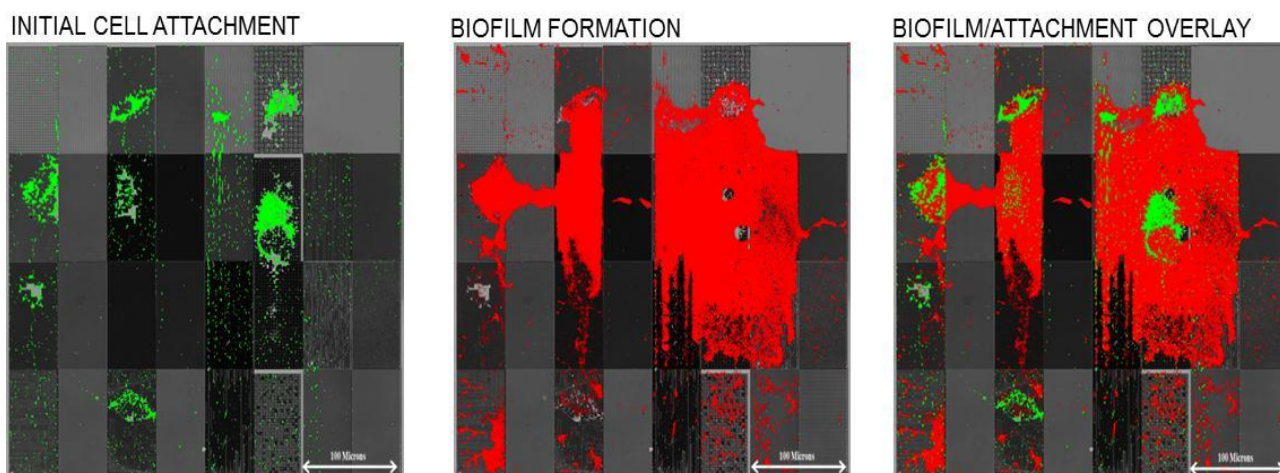
We have expanded this work to explore cell attachment and subsequent biofilm formation under fluid shear/flow conditions [53]. For this work we examined a novel set of engineered surface topographies, which ranged from 250 nm feature size/spacing, up to 2 μm feature size/spacing. This set of topographic features is shown in Figure 4, below. Uniquely, each topography is fabricated in both “raised” and “recessed” orientations. Thus, pillar-like structures with 2 μm feature size and 2 μm spacing are adjacent to “holes” with the same dimension and spacing.

**Figure 4.** Microscale and sub-micron topography for antifouling studies (from Ling *et al.* [53] with permission of World Scientific Publishing Company © 2012).



Using microfluidic devices similar to those shown in Figure 3, *Pseudomonas aeruginosa* cells were exposed to silicone-based replicas of the topographically defined surface (shown in Figure 4). Following the initial adhesion step, the surface was imaged (fluorescent microscopy) to observe the initial attachment locations for cells, which was then followed by a 24 h exposure to sterile growth media, under laminar flow conditions. This “outgrowth” step allowed surface-attached cells to form biofilms, which were then imaged at the end of the experiment. As shown in Figure 5, we found that the initial surface attachment was highly dependent upon the local topography.

**Figure 5.** Initial attachment and subsequent biofilm formation by *P. aeruginosa* on micron and sub-micron engineered surface topography (original data from Graham and Cady, figure adapted from our original work in Ling *et al.* [53]) with permission of World Scientific Publishing Company © 2012. The arrangement of topographical patterns in each panel is the same as shown in Figure 4. Scale bar is equal to 100 microns.



Subsequent biofilm formation occurred over these initial sites of attachment. Thus, we demonstrated that modulation of micro-scale and sub-micrometer topography can affect both initial attachment and resulting biofilm growth. Another observation was that cell attachment density was higher on “recessed” patterns *versus* “raised” patterns. For example, we observed much higher attachment to 0.75  $\mu\text{m}$  pillars than for 0.75  $\mu\text{m}$  holes. This may be due to the fact that the 0.5–1  $\mu\text{m}$  wide *P. aeruginosa* cells tended to wedge themselves between the “raised” features, as shown in Figure 6, which shows *P. aeruginosa* aligned and attached to the 0.75  $\mu\text{m}$  spaces in a line/space topography. The “recessed” features (holes) may be less accessible to cells, due to their small size. This is an area of further study in our laboratory, as we try to correlate the size, shape, and spacing of engineered topographies with bacterial attachment density. This is also an area of further study for the antifouling field in general. For instance, why do cells attach to certain topographical features and not others? This topic is explored in the following section.

**Figure 6.** *P. aeruginosa* attachment to 0.75  $\mu\text{m}$  spaces in a silicone-based 0.75  $\mu\text{m}$  line/0.75  $\mu\text{m}$  space pattern.



### 3. Pushing Antifouling Topography to the Nanoscale

Engineered micro and nanoscale surface topographies have been explored for reduction of biofouling and subsequent biofilm formation. To this end, Xu *et al.* hypothesized that surface textures with dimensions less than the size of a single bacterial cell could reduce the surface area accessible to bacteria, resulting in a decreased probability of interaction with, and attachment to, the material surface [81]. As a result, the flow of fluid over the material surface could remove bacteria from textured surfaces more efficiently than it would from a smooth surface, subsequently reducing cell attachment and biofilm formation. Accordingly, they examined bacterial surface adhesion and biofilm formation on textured surfaces with arrays of sub-micron diameter pillars (ranging from 400 to 500 nm). As stated above, the goal of using feature dimensions smaller than the size of the organism (less than 1  $\mu\text{m}$ ) was to minimize contact area between the bacterial cell and the substrate surface. Their experiments were carried out under the influence of physiologically-relevant fluid shear conditions. Their findings showed that bacterial cell attachment, and accordingly, biofilm formation was significantly reduced on the texturized surfaces, in comparison to that of the smooth surface. They also found this to be true under low fluid shear conditions.

While there remains ongoing research to understand bacterial cell attachment on engineered micrometer-scaled topographic features, and features with sub-micron dimensions (>100 nm), there is also an interest in examining attachment and biofilm formation on nanoscale sized features (<100 nm). Mechanisms underpinning attachment to nanoscale topographies for mammalian cells is a greatly studied area which has continued to foster significant findings and major contributions to the wealth of knowledge on eukaryotic cell behavior [82–85]. However, as Hsu *et al.* [48] have described, attachment phenomena for bacterial cells at the nanoscale is less understood, as relatively few reported works have explored the effects of nanoscale topography on bacterial attachment behavior and biofilm formation [23,49,54,86,87]. In fact, some work on bacterial attachment to nanoscale topography resulted in a higher degree of attachment to nanoscaled surfaces rather than planar or micron-scaled topography [88–91]. Other groups, however, have seen an antifouling effect on nanoscaled surfaces [23,92]. Albeit varied, bacterial cells clearly exhibit an attachment response to nanoscaled topography. It is essential to note that most of these aforementioned studies focus on nano-roughened,

nano-texturized, or nanoporous surfaces. Relatively few studies have addressed engineered nanoscale topography (containing well-defined features) [7,9].

Anselme *et al.* have provided some understanding of bacterial cell interactions at the nanoscale [7]. Much of their work is based on the premise that small (nanoscale) bacterial appendages (flagella, pili, fimbriae, *etc.*) can directly interact with nanoscale topographical features. They go on to state that bacteria typically have relatively rigid morphologies, due to their peptidoglycan based cell wall. Thus, in the presence of topographical features, they are not easily deformed (as mammalian cells would typically be) [7]. Instead, bacterial appendages are both small and relatively flexible, enabling them to probe nanoscale features [54,86,87]. Thus, these extracellular appendages could play a crucial role in attachment to surface features much smaller than the dimensions of the cells themselves. For example, fimbriae on certain bacteria can range from a few hundred nanometers to a few micrometers in length and have diameters that are less than 10 nm [7]. Bacterial flagella are considerably thicker than fimbriae (up to tens of nanometers in diameter), yet they too may play a crucial role in bacterial adhesion at the submicron and nanoscale dimensions [7].

In a similar approach, Hsu *et al.*, have explored bacterial attachment to nanoscale alumina surfaces [48]. Their work has shown that the size, type, and number of bacterial appendages play a key role in attachment to surfaces, and that there are key differences in attachment by different species of bacteria (related to their morphology and types of appendages) [48]. As compared to a smooth (control) surface, they found a greater degree of attachment of Gram-negative bacterial strains to nanoscale topography. Surprisingly, they found the exact opposite trend for Gram-positive strain. In addition, cell size appeared to play a role in surface attachment. As compared to the smooth (control) surface, cells attached to the nanoscaled surface were much larger. This work helps to expand our knowledge of how bacteria might interact with nanoscale features, and is complementary to the work by Anselme *et al.* [7].

Epstein *et al.* have also focused on nanoscale topography, through the exploitation of both nanostructural mechanics and geometry to control bacteria biofilm growth on surfaces. This was done through the use of a high aspect ratio (HAR) pillared nanostructure array [9]. Their orthogonal double-gradient fabricated array consisted of a pitch gradient ranging from 0.8 to 4.0  $\mu\text{m}$ , and an orthogonal nanopost diameter gradient from 300 nm to  $\sim 1 \mu\text{m}$ . They performed studies using *Pseudomonas aeruginosa* [90]. These HAR nano and microscale structures were shown to induce long-range spontaneous spatial patterning of *P. aeruginosa* cells while on the surface. This group has additionally found that substrate stiffness plays a role in bacterial attachment and biofilm formation [9]. They have determined that when the stiffness of their pillar-based nanostructures is reduced beyond a threshold value (*i.e.*, when the surfaces become softer), biofilm formation becomes drastically reduced. The authors state that these results are consistent with the mechanoselective adhesion of bacteria to surfaces. Overall, their research shows that the combinatorial effects of nanoscale surface patterning and modulating the stiffness of the nanoarray can be used to inhibit bacterial biofilm growth.

Bacterial attachment to engineered surface topography is clearly a burgeoning field within the antifouling community. However, relatively few articles have explored engineered topography within the nanoscale size regime. Possible explanations for this shortage could stem from limited access to the state of the art lithographic tools and techniques that are needed to fabricate nanoscale structures with high fidelity. One would presume that the same fabrication techniques used by other research groups to construct nanoscale topographies for studies with mammalian cells, could just as easily be adopted for

the use of bacterial cells. However, many of those nanostructured surfaces were fabricated with the intent of replicating the 3D scaffold-like structure of the extra cellular matrix (ECM) in efforts of promoting mammalian cell differentiation and proliferation [93–97]. This is quite different than the motivation for antifouling work, which focuses on limiting and preventing bacterial attachment to surfaces. Thus, additional studies will be needed to better understand what size thresholds may exist for bacteria to discriminate between relatively “smooth” surfaces and those with nanoscale topographical features. Further, more work is needed to elucidate the role of bacterial appendages on attachment and retention on surfaces, as well as subsequent biofilm formation. A likely outcome of such work will be the recognition of species to species and strain to strain differences in surface interactions, especially due to phenotypic changes between organisms.

#### **4. Conclusions and Future Perspectives**

Preventing bacterial attachment to surfaces is critical for multiple industries, as well as for the preservation of human health. This review attempts to summarize the various approaches taken to limit bacterial surface fouling, by engineering surface topography at the micro and nano-scale. While engineered topographies are clearly able to limit bacterial cell attachment (as well as attachment by other microorganisms), a universal model for effective antifouling topographies has yet to be developed. Approaches such as the Engineered Roughness Index (ERI) and the description of nanoforce gradients are the first steps towards establishing a correlation between the engineered topographical features and cell attachment. These models, however, do not universally explain the wide variety of antifouling properties, partially due to the fact that fouling is also highly dependent upon a host of other factors, including the microorganism in question. Clearly the size and spacing of topographic features has a direct effect on fouling, with surface features and spacing less than the size of the fouling organism being the most effective. Because microorganisms come in many different shapes, sizes, aspect ratios, and with a host of different surface appendages, we may never be able to derive a universal model for evaluating antifouling topographies. In light of this, a goal of this research community may be to correlate antifouling properties of engineered topographies with cell size and shape. This would provide an initial design parameter, enabling more detailed studies with organisms within each size/shape category. Such a model would provide a systematic approach to developing new antifouling topographies.

#### **Acknowledgments**

The authors would like to acknowledge the SUNY College of Nanoscale Science & Engineering for financial support of author Mary V. Graham.

#### **Conflicts of Interest**

The authors declare no conflict of interest.

## References

1. Davey, M.E.; O'Toole, G.A. Microbial biofilms: From ecology to molecular genetics. *Microbiol. Mol. Biol Rev.* **2000**, *64*, 847–867.
2. Hall-Stoodley, L.; Costerton, J.W.; Stoodley, P. Bacterial biofilms: From the natural environment to infectious diseases. *Nat. Rev. Microbiol.* **2004**, *2*, 95–108.
3. Flemming, H.C.; Wingender, J. The biofilm matrix. *Nat. Rev. Microbiol.* **2010**, *8*, 623–633.
4. Hetrick, E.M.; Shin, J.H.; Paul, H.S.; Schoenfisch, M.H. Anti-biofilm efficacy of nitric oxide-releasing silica nanoparticles. *Biomaterials* **2009**, *30*, 2782–2789.
5. Epstein, A.K.; Pokroy, B.; Seminara, A.; Aizenberg, J. Bacterial biofilm shows persistent resistance to liquid wetting and gas penetration. *Proc. Natl. Acad. Sci. USA* **2011**, *108*, 995–1000.
6. Lindsay, D.; von Holy, A. Bacterial biofilms within the clinical setting: What healthcare professionals should know. *J. Hosp. Infect.* **2006**, *64*, 313–325.
7. Anselme, K.; Davidson, P.; Popa, A.M.; Giazson, M.; Liley, M.; Ploux, L. The interaction of cells and bacteria with surfaces structured at the nanometre scale. *Acta Biomater.* **2010**, *6*, 3824–3846.
8. Chiappetta, D.A.; Degrossi, J.; Teves, S.; D'Aquino, M.; Bregni, C.; Sosnik, A. Triclosan-loaded poloxamine micelles for enhanced topical antibacterial activity against biofilm. *Eur. J. Pharm. Biopharm.* **2008**, *69*, 535–545.
9. Epstein, A.K.; Hochbaum, A.I.; Kim, P.; Aizenberg, J. Control of bacterial biofilm growth on surfaces by nanostructural mechanics and geometry. *Nanotechnology* **2011**, *22*, doi:10.1088/0957-4484/22/49/494007.
10. Jin, F.; Conrad, J.C.; Gibiansky, M.L.; Wong, G.C. Bacteria use type-IV pili to slingshot on surfaces. *Proc. Natl. Acad. Sci. USA* **2011**, *108*, 12617–12622.
11. Kouidhi, B.; Zmantar, T.; Hentati, H.; Bakhrouf, A. Cell surface hydrophobicity, biofilm formation, adhesives properties and molecular detection of adhesins genes in staphylococcus aureus associated to dental caries. *Microb. Pathog.* **2010**, *49*, 14–22.
12. Matsumura, T.; Iida, F.; Hirose, T.; Yoshino, M. Micro machining for control of wettability with surface topography. *J. Mater. Process. Technol.* **2012**, *212*, 2669–2677.
13. Newell, P.D.; Monds, R.D.; O'Toole, G.A. Lapd is a bis-(3',5')-cyclic dimeric gmp-binding protein that regulates surface attachment by pseudomonas fluorescens pf0–1. *Proc. Natl. Acad. Sci. USA* **2009**, *106*, 3461–3466.
14. Schumacher, J.F.; Aldred, N.; Callow, M.E.; Finlay, J.A.; Callow, J.A.; Clare, A.S.; Brennan, A.B. Species-specific engineered antifouling topographies: Correlations between the settlement of algal zoospores and barnacle cyprids. *Biofouling* **2007**, *23*, 307–317.
15. Singh, A.V.; Vyas, V.; Patil, R.; Sharma, V.; Scopelliti, P.E.; Bongiorno, G.; Podesta, A.; Lenardi, C.; Gade, W.N.; Milani, P. Quantitative characterization of the influence of the nanoscale morphology of nanostructured surfaces on bacterial adhesion and biofilm formation. *PLoS One* **2011**, *6*, e25029.
16. Somorjai, G.A.; Li, Y. Impact of surface chemistry. *Proc. Natl. Acad. Sci. USA* **2011**, *108*, 917–924.
17. Whitehead, K.A.; Colligon, J.S.; Verran, J. The production of surfaces of defined topography and chemistry for microbial retention studies, using ion beam sputtering technology. *Int. Biodeterior. Biodegrad.* **2004**, *54*, 143–151.

18. Khoo, X.; Grinstaff, M.W. Novel infection-resistant surface coatings: A bioengineering approach. *MRS Bull.* **2011**, *36*, 357–366.
19. Mauclair, L.; Brombacher, E.; Bunger, J.D.; Zinn, M. Factors controlling bacterial attachment and biofilm formation on medium-chain-length polyhydroxyalkanoates (mcl-phas). *Colloids Surf. B Biointerfaces* **2010**, *76*, 104–111.
20. Harris, L.G.; Richards, R.G. Staphylococci and implant surfaces: A review. *Injury* **2006**, *37*, S3–S14.
21. Wu, P.; Grainger, D.W. Drug/device combinations for local drug therapies and infection prophylaxis. *Biomaterials* **2006**, *27*, 2450–2467.
22. Hoiby, N.; Johansen, H.K.; Moser, C.; Song, Z.; Ciofu, O.; Kharazmi, A. *Pseudomonas aeruginosa* and the *in vitro* and *in vivo* biofilm mode of growth. *Microbes Infect.* **2001**, *3*, 23–35.
23. Puckett, S.D.; Taylor, E.; Raimondo, T.; Webster, T.J. The relationship between the nanostructure of titanium surfaces and bacterial attachment. *Biomaterials* **2010**, *31*, 706–713.
24. Cai, W.; Wu, J.; Xi, C.; Meyerhoff, M.E. Diazoniumdiolate-doped poly(lactic-co-glycolic acid)-based nitric oxide releasing films as antibiofilm coatings. *Biomaterials* **2012**, *33*, 7933–7944.
25. Faure, E.; Vreuls, C.; Falentin-Daudre, C.; Zocchi, G.; van de Weerd, C.; Martial, J.; Jerome, C.; Duwez, A.S.; Detrembleur, C. A green and bio-inspired process to afford durable anti-biofilm properties to stainless steel. *Biofouling* **2012**, *28*, 719–728.
26. Smith, A.W. Biofilms and antibiotic therapy: Is there a role for combating bacterial resistance by the use of novel drug delivery systems? *Adv. Drug Deliv. Rev.* **2005**, *57*, 1539–1550.
27. Carmen, J.C.; Roeder, B.L.; Nelson, J.L.; Ogilvie, R.L.; Robison, R.A.; Schaalje, G.B.; Pitt, W.G. Treatment of biofilm infections on implants with low-frequency ultrasound and antibiotics. *Am. J. Infect. Control.* **2005**, *33*, 78–82.
28. Cirioni, O.; Giacometti, A.; Ghiselli, R.; Kamysz, W.; Orlando, F.; Mocchegiani, F.; Silvestri, C.; Licci, A.; Chiodi, L.; Lukasiak, J.; *et al.* Citropin 1.1-treated central venous catheters improve the efficacy of hydrophobic antibiotics in the treatment of experimental staphylococcal catheter-related infection. *Peptides* **2006**, *27*, 1210–1216.
29. Hindi, K.M.; Ditto, A.J.; Panzner, M.J.; Medvetz, D.A.; Han, D.S.; Hovis, C.E.; Hilliard, J.K.; Taylor, J.B.; Yun, Y.H.; Cannon, C.L.; *et al.* The antimicrobial efficacy of sustained release silver-carbene complex-loaded l-tyrosine polyphosphate nanoparticles: Characterization, *in vitro* and *in vivo* studies. *Biomaterials* **2009**, *30*, 3771–3779.
30. Valappil, S.P.; Ready, D.; Abou Neel, E.A.; Pickup, D.M.; O'Dell, L.A.; Chrzanowski, W.; Pratten, J.; Newport, R.J.; Smith, M.E.; Wilson, M.; *et al.* Controlled delivery of antimicrobial gallium ions from phosphate-based glasses. *Acta Biomater.* **2009**, *5*, 1198–1210.
31. Malcolm, R.K.; McCullagh, S.D.; Woolfson, A.D.; Gorman, S.P.; Jones, D.S.; Cuddy, J. Controlled release of a model antibacterial drug from a novel self-lubricating silicone biomaterial. *J. Control. Release* **2004**, *97*, 313–320.
32. Pinto-Alphandary, H.; Andremont, A.; Couvreur, P. Targeted delivery of antibiotics using liposomes and nanoparticles: Research and applications. *Int J. Antimicrob Agents* **2000**, *13*, 155–168.
33. Tamilvanan, S.; Venkateshan, N.; Ludwig, A. The potential of lipid- and polymer-based drug delivery carriers for eradicating biofilm consortia on device-related nosocomial infections. *J. Control. Release* **2008**, *128*, 2–22.

34. Fatima, A.; Shyum-Naqvi, S.B.; Khaliq, S.A.; Perveen, S.; Yousuf, R.I.; Saeed, R. Staphylococcal resistance against five groups of life saving antibiotics in the year 2003–2005. *Pak. J. Pharm. Sci.* **2013**, *26*, 1137–1140.
35. Hui, C.; Lin, M.C.; Jao, M.S.; Liu, T.C.; Wu, R.G. Previous antibiotic exposure and evolution of antibiotic resistance in mechanically ventilated patients with nosocomial infections. *J. Crit. Care* **2013**, *28*, 728–734.
36. Rodriguez-Rojas, A.; Rodriguez-Beltran, J.; Couce, A.; Blazquez, J. Antibiotics and antibiotic resistance: A bitter fight against evolution. *Int. J. Med. Microbiol.* **2013**, *303*, 293–297.
37. Biswas, A.; Bayer, I.S.; Biris, A.S.; Wang, T.; Dervishi, E.; Faupel, F. Advances in top–down and bottom–up surface nanofabrication: Techniques, applications & future prospects. *Adv. Colloid Interface Sci.* **2012**, *170*, 2–27.
38. Burgoyne, H.A.; Kim, P.; Kolle, M.; Epstein, A.K.; Aizenberg, J. Screening conditions for rationally engineered electrodeposition of nanostructures (screen): Electrodeposition and applications of polypyrrole nanofibers using microfluidic gradients. *Small* **2012**, *8*, 3502–3509.
39. Epstein, A.K.; Aizenberg, J. Biomimetic nanostructured surfaces with designer mechanics and geometry for broad applications. *MRS Online Proc. Lib.* **2009**, *1236*, doi:10.1557/PROC-1236-SS09-07.
40. Foncy, J.; Cau, J.-C.; Bartual-Murgui, C.; François, J.M.; Trévisiol, E.; S é v é r a c, C. Comparison of polyurethane and epoxy resist master mold for nanoscale soft lithography. *Microelectr. Eng.* **2013**, *110*, 183–187.
41. Grinthal, A.; Kang, S.H.; Epstein, A.K.; Aizenberg, M.; Khan, M.; Aizenberg, J. Steering nanofibers: An integrative approach to bio-inspired fiber fabrication and assembly. *Nano Today* **2012**, *7*, 35–52.
42. Kim, B.; Kim, J.; Takama, N. Fabrication of nano-structures using inverse- $\mu$ CP technique with a flat PDMS stamp. *Sens. Actuat. A Phys.* **2007**, *136*, 475–483.
43. Kim, P.; Epstein, A.K.; Khan, M.; Zarzar, L.D.; Lipomi, D.J.; Whitesides, G.M.; Aizenberg, J. Structural transformation by electrodeposition on patterned substrates (steps): A new versatile nanofabrication method. *Nano Lett.* **2012**, *12*, 527–533.
44. Manabe, K.; Nishizawa, S.; Shiratori, S. Porous surface structure fabricated by breath figures that suppresses pseudomonas aeruginosa biofilm formation. *ACS Appl. Mater. Interfaces* **2013**, *5*, 11900–11905.
45. Pokroy, B.; Epstein, A.K.; Persson-Gulda, M.C.M.; Aizenberg, J. Fabrication of bioinspired actuated nanostructures with arbitrary geometry and stiffness. *Adv. Mater.* **2009**, *21*, 463–469.
46. Shao, G.; Wu, J.; Cai, Z.; Wang, W. Fabrication of elastomeric high-aspect-ratio microstructures using polydimethylsiloxane (pdms) double casting technique. *Sens. Actuat. A Phys.* **2012**, *178*, 230–236.
47. Wang, L.; Lin, C.; Yang, L.; Zhang, J.; Zheng, J. Preparation of nano/micro-scale column-like topography on pdms surfaces via vapor deposition: Dependence on volatility solvents. *Appl. Surf. Sci.* **2011**, *258*, 265–269.
48. Hsu, L.C.; Fang, J.; Borca-Tasciuc, D.A.; Worobo, R.W.; Moraru, C.I. Effect of micro- and nanoscale topography on the adhesion of bacterial cells to solid surfaces. *Appl. Environ. Microbiol.* **2013**, *79*, 2703–2712.

49. Ivanova, E.P.; Hasan, J.; Webb, H.K.; Gervinskas, G.; Juodkazis, S.; Truong, V.K.; Wu, A.H.; Lamb, R.N.; Baulin, V.A.; Watson, G.S.; *et al.* Bactericidal activity of black silicon. *Nat. Commun.* **2013**, *4*, doi:10.1038/ncomms3838.
50. Jeyachandran, Y.L.; Narayandass, S.K.; Mangalaraj, D.; Bao, C.Y.; Li, W.; Liao, Y.M.; Zhang, C.L.; Xiao, L.Y.; Chen, W.C. A study on bacterial attachment on titanium and hydroxyapatite based films. *Surf. Coat. Technol.* **2006**, *201*, 3462–3474.
51. Joo, H.-C.; Lim, Y.-J.; Kim, M.-J.; Kwon, H.-B.; Han, J.-H. Characterization on titanium surfaces and its effect on photocatalytic bactericidal activity. *Appl. Surf. Sci.* **2010**, *257*, 741–746.
52. Kargar, M.; Wang, J.; Nain, A.S.; Behkam, B. Controlling bacterial adhesion to surfaces using topographical cues: A study of the interaction of pseudomonas aeruginosa with nanofiber-textured surfaces. *Soft Matter* **2012**, *8*, 10254–10259.
53. Ling, J.F.; Graham, M.V.; Cady, N.C. Effect of topographically patterned poly(dimethylsiloxane) surfaces on pseudomonas aeruginosa adhesion and biofilm formation. *Nano LIFE* **2012**, *2*, doi:10.1142/S1793984412420044.
54. Rizzello, L.; Galeone, A.; Vecchio, G.; Brunetti, V.; Sabella, S.; Pompa, P.P. Molecular response of escherichia coli adhering onto nanoscale topography. *Nanosc. Res. Lett.* **2012**, *7*, 575:1–575:8.
55. Verran, J.; Packer, A.; Kelly, P.; Whitehead, K.A. Titanium-coating of stainless steel as an aid to improved cleanability. *Int. J. Food Microbiol.* **2010**, *141*, S134–S139.
56. Diaz, C.; Minan, A.; Schilardi, P.L.; Fernandez Lorenzo de Mele, M. Synergistic antimicrobial effect against early biofilm formation: Micropatterned surface plus antibiotic treatment. *Int. J. Antimicrob. Agents* **2012**, *40*, 221–226.
57. Epstein, A.K.; Wong, T.S.; Belisle, R.A.; Boggs, E.M.; Aizenberg, J. Liquid-infused structured surfaces with exceptional anti-biofouling performance. *Proc. Natl. Acad. Sci. USA* **2012**, *109*, 13182–13187.
58. Whitehead, K.A.; Verran, J. The effect of surface topography on the retention of microorganisms. *Food Bioprod. Process.* **2006**, *84*, 253–259.
59. Shi, X.; Zhu, X. Biofilm formation and food safety in food industries. *Trends Food Sci. Technol.* **2009**, *20*, 407–413.
60. Abban, S.; Jakobsen, M.; Jespersen, L. Attachment behaviour of escherichia coli k12 and salmonella typhimurium p6 on food contact surfaces for food transportation. *Food Microbiol.* **2012**, *31*, 139–147.
61. Schumacher, J.F.; Carman, M.L.; Estes, T.G.; Feinberg, A.W.; Wilson, L.H.; Callow, M.E.; Callow, J.A.; Finlay, J.A.; Brennan, A.B. Engineered antifouling microtopographies—Effect of feature size, geometry, and roughness on settlement of zoospores of the green alga ulva. *Biofouling* **2007**, *23*, 55–62.
62. Callow, M.E.; Jennings, A.R.; Brennan, A.B.; Seegert, C.E.; Gibson, A.; Wilson, L.; Feinberg, A.; Baney, R.; Callow, J.A. Microtopographic cues for settlement of zoospores of the green fouling alga enteromorpha. *Biofouling* **2002**, *18*, 229–236.
63. Schumacher, J.F.; Long, C.J.; Callow, M.E.; Finlay, J.A.; Callow, J.A.; Brennan, A.B. Engineered nanoforce gradients for inhibition of settlement (attachment) of swimming algal spores. *Langmuir* **2008**, *24*, 4931–4937.
64. Bhushan, B. Bioinspired structured surfaces. *Langmuir* **2012**, *28*, 1698–1714.

65. Malshe, A.; Rajurkar, K.; Samant, A.; Hansen, H.N.; Bapat, S.; Jiang, W. Bio-inspired functional surfaces for advanced applications. *CIRP Ann. Manuf. Technol.* **2013**, *62*, 607–628.
66. Wenzel, R.N. Resistance of solid surfaces to wetting by water. *Ind. Eng. Chem.* **1936**, *28*, 988–994.
67. Bico, J.; Marzolin, C.; Quere, D. Pearl drops. *Europhys. Lett.* **1999**, *47*, 743–744.
68. Bico, J.; Thiele, U.; Quéré, D. Wetting of textured surfaces. *Colloids Surfaces A Physicochem. Eng. Aspects* **2002**, *206*, 41–46.
69. Bico, J.; Tordeux, C.; Quere, D. Rough wetting. *Europhys. Lett.* **2001**, *55*, 214–220.
70. Cassie, A.B.D.; Baxter, S. Wettability of porous surfaces. *Trans. Faraday Soci.* **1944**, *40*, 546–551.
71. Quere, D. Rough ideas on wetting. *Phys. A Statist. Mechan. Appl.* **2002**, *313*, 32–46.
72. Long, C.J.; Schumacher, J.F.; Robinson, P.A., 2nd; Finlay, J.A.; Callow, M.E.; Callow, J.A.; Brennan, A.B. A model that predicts the attachment behavior of *Ulva linza* zoospores on surface topography. *Biofouling* **2010**, *26*, 411–419.
73. Graham, M.V.; Mosier, A.P.; Kiehl, T.R.; Kaloyeros, A.E.; Cady, N.C. Development of antifouling surfaces to reduce bacterial attachment. *Soft Matter* **2013**, *9*, 6235–6244.
74. Nain, A.S.; Sitti, M.; Jacobson, A.; Kowalewski, T.; Amon, C. Dry spinning based spinneret based tunable engineered parameters (step) technique for controlled and aligned deposition of polymeric nanofibers. *Macromol. Rapid Commun.* **2009**, *30*, 1406–1412.
75. Perni, S.; Prokopovich, P. Micropatterning with conical features can control bacterial adhesion on silicone. *Soft Matter* **2013**, *9*, 1844–1851.
76. Chung, K.K.; Schumacher, J.F.; Sampson, E.M.; Burne, R.A.; Antonelli, P.J.; Brennan, A.B. Impact of engineered surface microtopography on biofilm formation of staphylococcus aureus. *Biointerphases* **2007**, *2*, 89–94.
77. Anstead, G.M.; Cadena, J.; Javeri, H. Treatment of infections due to resistant staphylococcus aureus. *Methods Mol. Biol.* **2014**, *1085*, 259–309.
78. Reddy, S.T.; Chung, K.K.; McDaniel, C.J.; Darouiche, R.O.; Landman, J.; Brennan, A.B. Micropatterned surfaces for reducing the risk of catheter-associated urinary tract infection: An *in vitro* study on the effect of sharklet micropatterned surfaces to inhibit bacterial colonization and migration of uropathogenic escherichia coli. *J. Endourol.* **2011**, *25*, 1547–1552.
79. Jones, G.L.; Russell, A.D.; Caliskan, Z.; Stickler, D.J. A strategy for the control of catheter blockage by crystalline proteus mirabilis biofilm using the antibacterial agent triclosan. *Eur. Urol.* **2005**, *48*, 838–845.
80. Epstein, A.K.; Hong, D.; Kim, P.; Aizenberg, J. Biofilm attachment reduction on bioinspired, dynamic, micro-wrinkling surfaces. *New J. Phys.* **2013**, *15*, 095018.
81. Xu, L.C.; Siedlecki, C.A. Submicron-textured biomaterial surface reduces staphylococcal bacterial adhesion and biofilm formation. *Acta Biomater.* **2012**, *8*, 72–81.
82. Curtis, A. Tutorial on the biology of nanotopography. *IEEE Trans. Nanobiosci.* **2004**, *3*, 293–295.
83. Dalby, M.J.; Riehle, M.O.; Sutherland, D.S.; Agheli, H.; Curtis, A.S. Changes in fibroblast morphology in response to nano-columns produced by colloidal lithography. *Biomaterials* **2004**, *25*, 5415–5422.
84. Flemming, R.G.; Murphy, C.J.; Abrams, G.A.; Goodman, S.L.; Nealey, P.F. Effects of synthetic micro- and nano-structured surfaces on cell behavior. *Biomaterials* **1999**, *20*, 573–588.

85. Martines, E.; McGhee, K.; Wilkinson, C.; Curtis, A. A parallel-plate flow chamber to study initial cell adhesion on a nanofeatured surface. *IEEE Trans. Nanobiosci.* **2004**, *3*, 90–95.
86. Dáz, C.; Schilardi, P.L.; Salvarezza, R.C.; Fernández Lorenzo de Mele, M. Nano/microscale order affects the early stages of biofilm formation on metal surfaces. *Langmuir* **2007**, *23*, 11206–11210.
87. Rizzello, L.; Sorce, B.; Sabella, S.; Vecchio, G.; Galeone, A.; Brunetti, V.; Cingolani, R.; Pompa, P.P. Impact of nanoscale topography on genomics and proteomics of adherent bacteria. *ACS Nano* **2011**, *5*, 1865–1876.
88. Mitik-Dineva, N.; Wang, J.; Stoddart, P.R.; Crawford, R.J.; Ivanova, E.P. Nano-Structured Surfaces Control Bacterial Attachment. In Proceedings of the IEEE ICONN 2008 International Conference on Nanoscience and Nanotechnology, Melbourne, Victoria, Australia, 25–29 February 2008; pp. 113–116.
89. Mitik-Dineva, N.; Wang, J.; Truong, V.K.; Stoddart, P.R.; Malherbe, F.; Crawford, R.J.; Ivanova, E.P. Differences in colonisation of five marine bacteria on two types of glass surfaces. *Biofouling* **2009**, *25*, 621–631.
90. Mulcahy, L.R.; Isabella, V.M.; Lewis, K. *Pseudomonas aeruginosa* biofilms in disease. *Microb. Ecol.* **2013**, in press.
91. Park, M.R.; Banks, M.K.; Applegate, B.; Webster, T.J. Influence of nanophase titania topography on bacterial attachment and metabolism. *Int. J. Nanomed.* **2008**, *3*, 497–504.
92. Diaz, C.; Schilardi, P.L.; dos Santos Claro, P.C.; Salvarezza, R.C.; Fernandez Lorenzo de Mele, M.A. Submicron trenches reduce the *pseudomonas fluorescens* colonization rate on solid surfaces. *ACS Appl. Mater. Interfaces* **2009**, *1*, 136–143.
93. Yim, E.K.; Darling, E.M.; Kulangara, K.; Guilak, F.; Leong, K.W. Nanotopography-induced changes in focal adhesions, cytoskeletal organization, and mechanical properties of human mesenchymal stem cells. *Biomaterials* **2010**, *31*, 1299–1306.
94. Bae, D.; Moon, S.-H.; Park, B.G.; Park, S.-J.; Jung, T.; Kim, J.S.; Lee, K.B.; Chung, H.-M. Nanotopographical control for maintaining undifferentiated human embryonic stem cell colonies in feeder free conditions. *Biomaterials* **2014**, *35*, 916–928.
95. Wang, P.Y.; Yu, J.; Lin, J.H.; Tsai, W.B. Modulation of alignment, elongation and contraction of cardiomyocytes through a combination of nanotopography and rigidity of substrates. *Acta Biomater.* **2011**, *7*, 3285–3293.
96. Kim, H.N.; Jiao, A.; Hwang, N.S.; Kim, M.S.; Kang do, H.; Kim, D.H.; Suh, K.Y. Nanotopography-guided tissue engineering and regenerative medicine. *Adv. Drug Deliv. Rev.* **2013**, *65*, 536–558.
97. Kim, H.N.; Hong, Y.; Kim, M.S.; Kim, S.M.; Suh, K.Y. Effect of orientation and density of nanotopography in dermal wound healing. *Biomaterials* **2012**, *33*, 8782–8792.